JOURNAL OF BACTERIOLOGY, Oct. 1995, p. 5628–5635 Vol. 177, No. 19
0021-9193/95/$04.00+0
Copyright © 1995, American Society for Microbiology

Identification and Characterization of Sporulation Gene *spoVS* from *Bacillus subtilis*

ORNA RESNEKOV, ADAM DRIKS,† AND RICHARD LOSICK*

Department of Molecular and Cellular Biology, The Biological Laboratories, Harvard University, Cambridge, Massachusetts 02138

Received 23 May 1995/Accepted 23 July 1995

We report the identification and characterization of an additional sporulation gene from *Bacillus subtilis* called *spoVS*, which is induced early in sporulation under the control of σ^H. We show that *spoVS* is an 86-codon-long open reading frame and is capable of encoding a protein of 8,796 Da which exhibits little similarity to other proteins in the databases. Null mutations in *spoVS* have two contrasting phenotypes. In otherwise wild-type cells they block sporulation at stage V, impairing the development of heat resistance and coat assembly. However, the presence of a *spoVS* mutation in a *spoIIB spoVG* double mutant (which is blocked at the stage [II] of polar septation) acts as a partial suppressor, allowing sporulation to advance to a late stage. The implications of the contrasting phenotypes are discussed in the context of the formation and maturation of the polar septum.

During the developmental pathway of sporulation in *Bacillus subtilis*, cells undergo a series of elaborate morphological transformations (18, 25), commencing with the formation of an asymmetrically positioned septum. The sporulation septum partitions the developing cell (or sporangium) into two cells of unequal size, known as the forespore (the smaller cell) and the mother cell. Following septum formation, the membrane of the mother cell migrates around the forespore, engulfing the smaller cell and pinching it off as a free protoplast within the mother cell. Further events in spore formation include the deposition of cortex and primordial cell wall between the membranes that separate the engulfed forespore from the surrounding mother cell, dehydration of the forespore cytoplasm (which will become the spore core), and assembly around the developing spore of a thick protein coat. Finally, upon maturation, the spore is released from the sporangium by lysis of the mother cell.

Here we are concerned with events involved in the formation and maturation of the sporulation septum, which differs in two important respects from the septum of vegetative cells undergoing binary fission. First, sporulation septum placement is polar, while in binary fission, the septum is positioned medially. Second, shortly after the formation of the sporulation septum, the layer of cell wall between the membranes of the septum is observed to undergo dissolution (13). This degradation starts in the middle of the septum and proceeds towards but does not reach the layer of cell wall that surrounds the sporangium. Thus, the resulting products of polar septation are retained side by side within the sporangium. In contrast, during binary fission, autolysis begins at the cell wall and proceeds towards the middle of the septum. Rather than degrading the wall, this process splits the wall in two along its length, releasing the daughter cells from each other.

Mutations in several sporulation genes that cause cells to be blocked at substages of the process of septum formation and maturation have been identified. These can be classified into early-acting mutations, which allow the sporangium to form an asymmerically positioned septum (*spoIIE* [13], *spoIIAC* [13], *spoIIG* [13], and *spoIIB spoVG* [21]) but are blocked in subsequent morphogenesis, and later-acting mutations, which allow degradation of the cell wall in the sporulation septum to commence but prevent engulfment (*spoIID* [4], *spoIIM* [32], and *spoIIP* [9]). In the present study, we have investigated the roles of *spoIIB* and *spoVG* in sporulation septum formation. Mutations in either *spoIIB* or *spoVG* alone have a minimal effect on sporulation (21, 30). However, when the mutations are combined, the efficiency of sporulation is reduced 10,000-fold, with blockage occurring after the septum is formed but prior to full removal of wall material from between the septal membranes (21). This synergy suggests that *spoIIB* and *spoVG* participate in functionally redundant pathways that are critical to the maturation of the sporulation septum. Little is known about the function of *spoVG* (12), but the similarity of the C-terminal region of SpoIIB to the C-terminal regions of two cell wall hydrolases from *Bacillus licheniformis* (CwlM [16]) and *B. subtilis* (CwlC [15]) suggests that *spoIIB* may be involved in the degradation of septal cell wall material (15, 21).

To study the roles of *spoIIB* and *spoVG* in sporulation septum formation, we sought extragenic suppressor mutations that would allow the doubly mutant cells to sporulate. Here we report the isolation of suppressor mutations that lie in a newly identified, developmentally regulated open reading frame (ORF), which we have named *spoVS*. Ironically, mutations in *spoVS*, which are capable of partially suppressing the *spoIIB spoVG* defect, impair sporulation at a late stage in otherwise wild-type cells. The implications for these findings in the process of formation and maturation of the polar septum are discussed.

MATERIALS AND METHODS

Bacterial strains. The *B. subtilis* strains used in this study are listed in Table 1. The *Escherichia coli* strain used was TG1 (except as indicated).

Plasmids. Plasmid pOR100 was created by moving the 2-kb *Hin*dIII insert from pLZ100 (35) into pER19 (a pUC19 derivative containing a *cat* cassette) (27) digested with *Hin*dIII. The orientation of the insert was determined by restriction digests.

Plasmid pOR175 was created by subcloning a fragment of pOR114 (see below under Chromosome Walking). pOR114 was digested with *Sac*I, and a 3-kb fragment was gel purified. The 3-kb fragment was digested with *Pst*I to generate

* Corresponding author. Mailing address: Department of Molecular and Cellular Biology, Harvard University, 16 Divinity Avenue, Cambridge, MA 02138. Phone: (617) 495-1774. Fax: (617) 496-4642.

† Present address: Department of Microbiology and Immunology, Stritch School of Medicine, Loyola University, Maywood, IL 60153.

TABLE 1. *B. subtilis* strains[a]

Strain	Relevant genotype or description	Source (reference)
AB408	P_{spac}-*spo0H* (*cat*)	Laboratory stock (A. Bosma)
OR57	*spoVG*::Tn*917*ΩHU265	KS265 (21)
OR61	*spoIIB*Δ::*erm*	PM735 (21)
OR121	*spoIIB*::*spoIIB-lacZ*Ω*cat*	Laboratory stock, PM608
OR125	*spoIIB*::*spoIIB-lacZ*Ω*cat spoVG*::Tn*917*ΩHU265	Laboratory stock, PM671
OR129	*spoIIB*Δ::*erm spoVG*::Tn*917*ΩHU265	PM740 (21)
OR565	*cotE*::pOR100	PY79 × pOR100[b]
OR639	*amyE*::*spoVS*$^+$	PY79 × pOR187[c]
OR641	*spoVS*::pOR191	PY79 × pOR191[b]
OR650	*amyE*::*spoVS-lacZ*	PY79 × pOR223[c]
OR652	*spo0H*Δ*Hin*dIII *amyE*::*spoVS-lacZ*	RL56 × DNA OR650
OR654	*spoIIAC1 amyE*::*spoVS-lacZ*	RL60 × DNA OR650
OR656	*spoIIG55 amyE*::*spoVS-lacZ*	RL67 × DNA OR650
OR660	*amyE*::*spoVS-lacZ*(*spc*)	OR650 × pJL62 (17)[c]
OR661	*spoVS*Δ::*spc*	PY79 × pOR235[c]
OR671	P_{spac}-*spo0H* (*cat*) *amyE*::*spoVS-lacZ* (*spc*)	OR660 × DNA AB408
OR683	*spoIIB*::*spoIIB-lacZ*Ω*cat spoVG*::Tn*917*ΩHU265 *spoVS*Δ::*spc*	OR125 × DNA OR661
OR696	*amyE*::*spoVS*11-4	PY79 × pOR245[c]
OR708	*spoVS*Δ::*spc amyE*::*spoVS*$^+$	OR661 × DNA OR639
OR710	*spoVS*Δ::*spc amyE*::*spoVS*11-4	OR661 × DNA OR696
OR732	*spoVS*8-9	This study
OR733	*spoVS*9-4	This study
OR734	*spoVS*11-4	This study
PY78[d]	*glnA*100	Laboratory stock, RL4
PY79	Prototrophic	Laboratory stock
RL48[e]	*cotE*Δ::*cat trpC2*	Laboratory stock
RL52[e]	*cotC*::*cat trpC2*	Laboratory stock
RL56	*spo0H*Δ*Hin*dIII	Laboratory stock
RL60	*spoIIAC1*	Laboratory stock
RL67	*spoIIG55*	Laboratory stock
RL215[f]	*spoIIG*::pDG261	Laboratory stock
RL340[f]	*zdi-82*::Tn*917 trpC2* SPβc2	Laboratory stock (34)

[a] All strains are congenic with PY79 except as noted.
[b] Introduced by a single recombination event (Campbell-like).
[c] Introduced by a double recombination (marker replacement) event.
[d] Congenic with CU1769.
[e] Congenic with PY17.
[f] Congenic with strain 168.

two fragments of 2 and 1 kb. The 2-kb fragment was gel purified and cloned in pER19 (27) digested with *Pst*I and *Sac*I to generate pOR175. A similar strategy was followed to subclone the *spoVS* mutations from plasmids pOR162, pOR194, and pOR198 (see Chromosome Walking) to generate plasmids pOR180 (*spoVS*11-4), pOR210 (*spoVS*8-9), and pOR213 (*spoVS*9-4).

Plasmid pOR191 was created by subcloning a 200-bp *Taq*I fragment (internal to *spoVS*) from pOR175. The orientation of the fragment was determined by restriction digests and sequencing.

Plasmid pOR235 was used to construct a *spoVS* null mutation in the *B. subtilis* chromosome. The plasmid was built in two steps. In the first step, pOR175 (prepared in JM110, a *dam* host) was digested with *Sac*I and *Bcl*I to generate a fragment of about 0.8 kb, which was cloned into pJL74 (17) that had been digested with *Bam*HI and *Sac*I, creating pOR225. In the second step, pOR191 was digested with *Pst*I and *Sma*I to generate a fragment of about 0.2 kb that was cloned into pOR225 that had been digested with *Pst*I and *Eco*RV, generating pOR235. Before transformation of *B. subtilis*, pOR235 was linearized with *Ava*II.

To create a plasmid capable of introducing a copy of *spoVS* at the *amyE* locus, a 2-kb *Hin*dIII-*Eco*RI fragment of pOR175 was cloned in pDG364 (11), creating pOR187. An analogous plasmid carrying the *spoVS*11-4 mutant form of *spoVS* was called pOR245. To linearize either pOR187 or pOR245, the plasmids were digested with *Bgl*II.

To create a plasmid that allowed the placement of a *spoVS-lacZ* transcriptional fusion at the *amyE* locus, a 1.2-kb *Eco*RI-*Cla*I fragment of pOR175 was first cloned into pER19 (27), digested with *Acc*I and *Eco*RI, to generate pOR219. pOR219 was then digested with *Eco*RI and *Hin*dIII, and the resulting 1.2-kb fragment was inserted into pDG268 (11), generating pOR223. To linearize pOR223, it was digested with *Bgl*II.

Plasmid p5E2 was a gift of H. Paulus (2).

Plasmids pJL62 and pJL64 were a gift of J. R. LeDeaux (17). pJL62 was linearized with *Pst*I.

General methods. (i) Growth and media. For the routine growth of *B. subtilis* and *E. coli*, LB medium was used (19). Sporulation of *B. subtilis* strains was tested in DS medium (11); the start of sporulation (T_0) was defined as the end of exponential growth. In order to induce σ^H activity during growth, *B. subtilis* was grown in 2×YT medium (19). Transformation of *B. subtilis* and *E. coli* was performed as described before (3, 8). Antibiotics were used at the following concentrations: chloramphenicol (Cm) at 5 μg/ml; erythromycin and lincomycin together (MLS) at 1 and 25 μg/ml, respectively; spectinomycin (Spc) at 100 μg/ml; and ampicillin (Amp) at 100 μg/ml. Selection for prototrophy in *B. subtilis* was done on TSS agar plates with the necessary amino acid supplements at 50 μg/ml (11).

(ii) β-Galactosidase assays. β-Galactosidase activity was determined as described before (22), with toluene used to permeabilize the cells.

(iii) NTG mutagenesis and isolation of *spoVS* mutants. To isolate *spoVS* mutants, an exponentially growing culture of OR129 (*spoVG*::Tn*917 spoIIB*Δ::*erm*) was washed in warm 0.15 M NaCl–0.01 M sodium citrate, pH 7.0 (SC buffer) and treated with either 25 or 50 μg of *N*-methyl-*N*′-nitro-*N*-nitrosoguanidine (NTG) per ml for 10 min at 37°C with slow shaking. The cells were washed twice in SC buffer and plated on DS agar, and mutants were screened for visually. By this method, we were able to obtain 10 colonies that were light brown. Phase-contrast microscopy showed that the cells produced prespores and immature spores. We were unable to obtain any chloroform-resistant colonies (11) after mutagenesis. In order to separate multiple mutations that might be in the DNA of the mutagenized cells, chromosomal DNA was prepared from each of the 10 colonies and used to transform strain OR57 (*spoVG*::Tn*917*) in congression with DNA from a *spoIIB* null mutant (*spoIIB-lacZ*Ω*Cm*). In all cases congressants that were Cm^r and MLS^r and that gave rise to light brown colonies containing prespores and immature spores were recovered. Chromosomal DNA was prepared separately from 3 of the 10 colonies (that were from separate mutagenesis reactions in order to exclude siblings), and the mutations were introduced by congression into PY78 (*glnA*100), selecting for prototrophy on minimal agar. In all cases, rare congressants that were Cm^s and MLS^s on LB agar and contained a mutation(s) in a sporulation gene, as assessed by their phenotype on DS agar, were recovered. In order to check that these mutations were the ones that

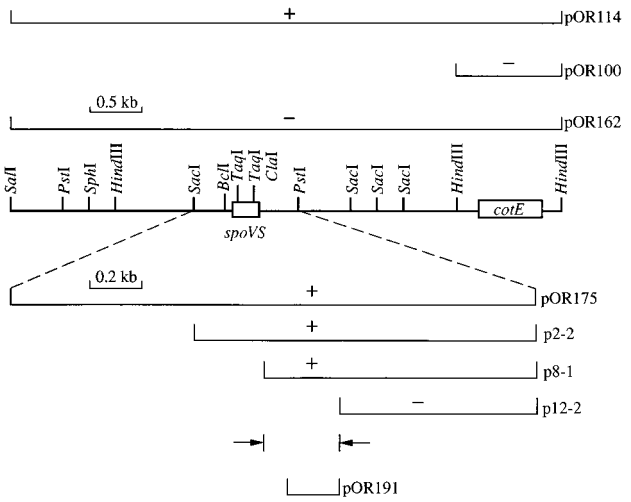

FIG. 1. Physical map of the *spoVS* region of the chromosome. Presented is a restriction map of the region surrounding *spoVS*; the predicted ORFs for *spoVS* and *cotE* are shown with boxes. In both cases, the direction of transcription is from left to right. Above and below the restriction map are the names of plasmids; the region of chromosomal DNA that each plasmid contains is indicated by a line. The ability of each plasmid to rescue the *spoVS*8-9, *spoVS*9-4, and *spoVS*11-4 mutations when integrated into the chromosome is indicated as + or −. Plasmid pOR114 was cloned from PY79, and pOR162 was cloned from the *spoVS*11-4 mutant (see Results). Note the change in scale above and below the restriction map. The region whose boundaries are indicated by two arrows and two bars represents the interval within which the *spoVS* mutations are expected to lie (see Results). Plasmid pOR191 is predicted to disrupt *spoVS* when integrated into the chromosome (see Materials and Methods and Results).

allowed OR129 cells to progress past stage II of sporulation and not simply mutations in sporulation genes that were not involved in this process, reconstitution experiments were performed by introducing *spoIIB* and *spoVG* null mutations by congression into each of the three strains. In all cases, the resulting Cm^r MLS^r cells gave rise to colonies that were light brown and produced prespores and immature spores when grown on DS agar. We inferred that the mutation(s) in strains *spoVS*8-9, *spoVS*9-4, and *spoVS*11-4 were in loci that were involved in sporulation and which allowed OR129 cells to progress past stage II of sporulation. We used these strains and the fact that they had a sporulation phenotype to our advantage to map the mutation(s).

(iv) Nucleotide sequence analysis. Nucleotide sequence analysis was performed by using dideoxy-nucleotide chain termination (31), double-stranded DNA templates, and the Sequenase kit (U.S. Biochemicals). The sequence of both strands of the sequence shown was determined. Sequencing of the wild type was initially performed on templates generated by exonuclease III digestion of pOR175 (these are listed in order of decreasing size of insert: p2-2, p4-1, p8-1, p10-3, p12-2, and p6-4) (for generation of the templates, see below) with a primer complementary to *lacZ* (OL62: 5′-GGG GAT GTG CTG CAA GGC-3′) and the M13/pUC reverse sequencing primer 1201 (5′-AAC AGC TAT GAC CAT G-3′). The wild-type sequence was confirmed by sequencing the region shown in Fig. 2 on both strands with synthetic primers. The sequence of the three mutants was obtained by using plasmids pOR180 (*spoVS*11-4), pOR210 (*spoVS*8-9), and pOR213 (*spoVS*9-4) and the same primers.

(v) Exonuclease deletion templates. Plasmid pOR175 was used to prepare exonuclease III-deleted templates. The plasmid was digested with *Eco*RI, and the ends were filled in with α-phosphorothioate nucleotides, then the plasmid was digested with *Ecl*136II, and deletion templates were prepared by using the Erase-a-base system (Promega). Following transformation, the resulting plasmids were linearized, separated by size on agarose gels, and used for nucleotide sequence analysis and transformation experiments. Primarily three plasmids from the deletion series were used: p2-2, p8-1, and p12-2. Their insert endpoints are diagrammed in Fig. 1.

(vi) Chromosomal DNA. Chromosomal DNA from *B. subtilis* was prepared as described before (11).

(vii) Amylase activity. Amylase activity was examined by growing cells on 1% starch plates overnight and then staining the agar with Gram's iodine solution (Sigma HT90-2-32).

(viii) Electron microscopy. Cells were harvested at 24 h after the start of sporulation and fixed and sectioned for electron microscopy as described before (20).

Genetic mapping. For mapping the *spoVS* mutations, we used PBS1-mediated generalized transduction (11) to determine the linkage of the *spoVS* mutations to a mapped set of cryptic Tn*917* insertions (34). We initially used mutant *spoVS*8-9 and then confirmed the analysis in mutants *spoVS*11-4 and *spoVS*9-4. We found 34% linkage to one of the insertions, *zdi-82*::Tn*917* (RL340), which had been mapped to 140° on the *B. subtilis* chromosome (34). Three other markers in the same region of the chromosome also showed linkage to *spoVS*8-9: a silent insertion near *spoIIG* (RL215, 135°) exhibited 15% linkage; a marker in the gene for *cotE* (RL48, 150°) showed 90% linkage; and a marker in the gene for *cotC* (RL52, 168°) showed 26% linkage. Three-factor crosses showed that the gene order was *zdi-82*::Tn*917 spoVS*8-9 *cotE* and *zdi-82*::Tn*917 dapA spoVS*8-9, using a silent insertion near *dapA* (144°, p5E2) (2). DNA-mediated transformation analysis showed that *spoVS*8-9 was 20% linked to *cotE*, while mutations *spoVS*9-4 and *spoVS*11-4 were 33 and 27% linked to the same marker, respectively.

Chromosome walking. Plasmid pOR100 (that included *cotE* and flanking DNA) was integrated into PY79 by a single-reciprocal recombination event, and chromosomal DNA was prepared from the resulting strain (OR565). In order to clone DNA upstream of the *Hin*dIII fragment, OR565 chromosomal DNA was cut with a variety of enzymes separately, and each digestion reaction product was ligated (1.5 μg of DNA per 300 μl of ligation reaction mix) and transformed into TG1. Only ligation products which contained an *E. coli* origin of replication were able to replicate. The resulting plasmids were tested for the size of their inserts. The largest insert originated from a *Sal*I digest of chromosomal DNA from OR565 and contained a 10.5-kb insert which included the *cotE* gene (pOR114). DNA-mediated transformation experiments showed that this plasmid was able to correct the *spoVS* mutations about 50% of the time, and the plasmid was used as a starting point to subclone and sequence *spoVS*. A similar chromosome walk was performed in *spoVS* mutants 8-9, 9-4, and 11-4 in order to clone the *spoVS* mutations and resulted in plasmids pOR194 (*spoVS*8-9), pOR198 (*spoVS*9-4), and pOR162 (*spoVS*11-4).

Preparation and analysis of RNA. RNA was prepared (26) from strains PY79 and OR661 at the indicated times and analyzed by Northern (RNA) blot hybridization (19) on 1.5% agarose–formaldehyde gels with 10 μg of RNA per sample. RNA markers from Bethesda Research Laboratories were used for size determinations. The RNA was blotted to Hybond-N filters and processed according to the manufacturer's instructions. The probe used for hybridization was a 200-bp *Taq*I fragment (Fig. 1) of *spoVS* that was labeled by random priming (Pharmacia). Following hybridization, the blot was stained with methylene blue to visualize the rRNA (which showed that approximately equal amounts of RNA were loaded per lane) and the RNA markers (24).

Nucleotide accession number. The sequence shown in Fig. 2 has been assigned accession number U27501.

RESULTS

Suppressor mutations that allow *spoIIB spoVG* mutant cells to advance beyond stage II. To study the role of *spoIIB* and *spoVG* in sporulation septum formation, we sought extragenic suppressor mutations that would allow the doubly mutant cells to progress beyond morphological stage II. Strains that are doubly mutant for *spoIIB* and *spoVG* (e.g., OR129) produce translucent colonies as a result of cell lysis when grown on solid sporulation (DS) medium, whereas wild-type cells produce opaque colonies that become brown as a result of sporulation pigment formation. Among about 50,000 colonies of nitrosoguanidine-mutagenized OR129, 10 mutants that were more opaque and brown than the parent strain were found. Phase-contrast microscopy showed that the 10 mutants were capable of producing prespores and immature spores which were less refractile than those of the wild type. Also, the mutants were 100- to 3,000-fold more capable of producing heat-resistant spores than the original *spoVG spoIIB* double mutant but less capable than the wild type. These suppressors were called *spoVS* mutations for reasons that will become apparent below.

All of the *spoVS* mutations were individually moved by congression (see Materials and Methods) into unmutagenized cells of *spoVG* mutant OR57 (*spoVG*::Tn*917*, MLS^r), concurrently introducing a *spoIIB* null mutation (*spoIIB-lacZ*Ω*cat*). In all cases, congressants that were Cm^r and MLS^r and produced light brown opaque colonies containing prespores and immature spores could be recovered. Also, the congressants were more capable (100- to 3,000-fold) of producing heat-resistant spores than was the *spoVG spoIIB* double mutant (OR125) but less capable than the wild type. These findings

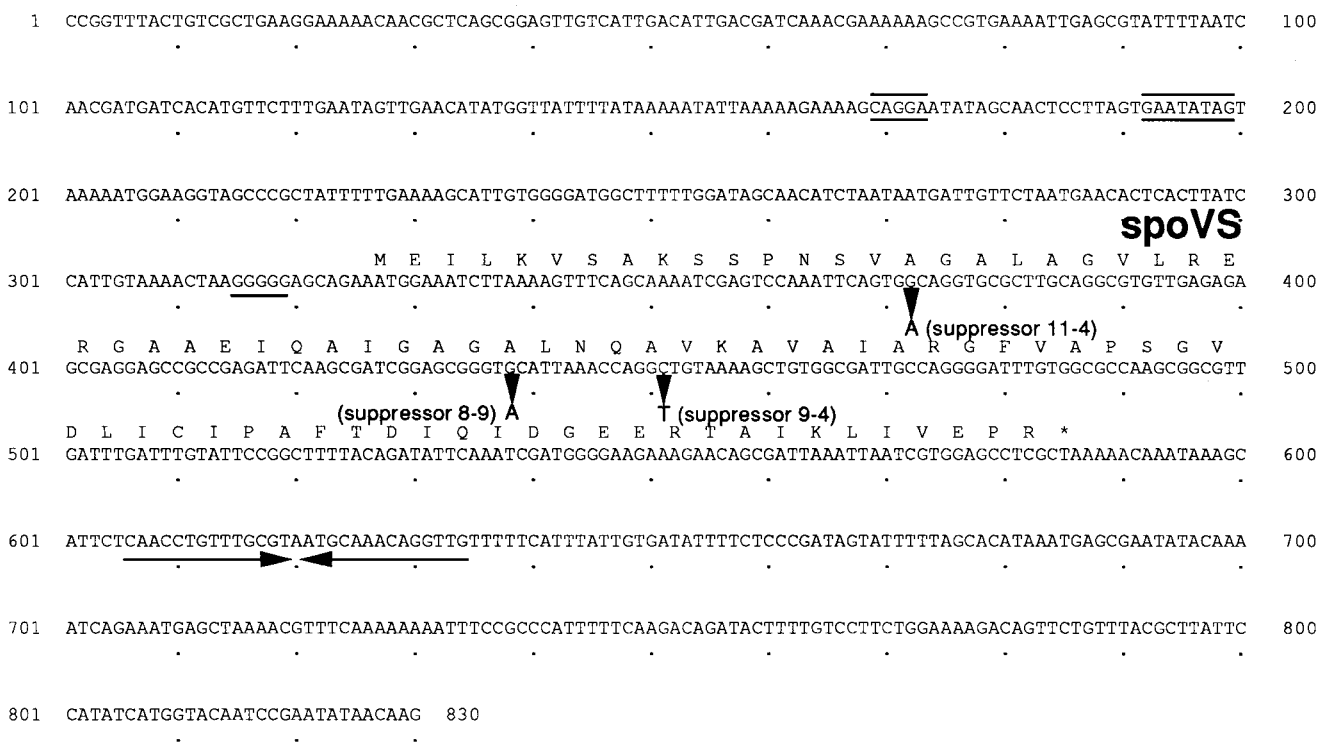

FIG. 2. Nucleotide sequence of the *spoVS* region of the chromosome. The figure shows the nucleotide sequence of *spoVS* and surrounding DNA. The predicted amino acid sequence of SpoVS is shown in the one-letter code positioned above the first nucleotide of each codon; * represents a stop codon. The nucleotide sequence shown corresponds to the region represented by the left-hand boundary of p2-2 (Fig. 1) to about 240 nucleotides downstream of the *spoVS* ORF (see Materials and Methods). A proposed ribosome-binding site is underlined, the proposed −10 and −35 regions of a σ^H promoter are both under- and overlined, and an inverted repeat which could serve as a rho-independent transcriptional terminator is indicated with horizontal arrows. The point mutations introduced by *spoVS*8-9, *spoVS*9-4, and *spoVS*11-4 are shown beneath vertical arrows (for the amino acid changes introduced as a result of the point mutations, see Results).

indicated that the suppressor phenotypes result from one or more closely linked mutations.

Mapping the *spoVS* mutations. Three of the *spoVS* mutations (*spoVS*8-9, *spoVS*11-4, and *spoVS*9-4), each derived from a separate mutagenesis experiment, were moved by congression into the Spo^+ strain PY78 (*glnA*). Congressants that were Gln^+, Cm^s, and MLS^s were readily recovered but were impaired in sporulation. This finding (as will be confirmed below) indicated that the suppressor mutations impair sporulation in the absence of mutations in *spoIIB* and *spoVG*. We took advantage of this sporulation phenotype to map the locations of the *spoVS* mutations on the chromosome by phage PBS1-mediated transduction and DNA-mediated transformation. All three of the mutations were found to map (by transduction) at approximately 149°, the gene order being *cotE spoVS dapGA*. The *spoVS* mutations were 89 to 93% linked by transduction and 20 to 33% linked by transformation with a drug resistance marker (Cm) at *cotE* (RL48, *cotE*Δ::*cat*).

Cloning and sequencing *spoVS* and its mutant alleles. To locate the *spoVS* mutations more precisely, we took advantage of the existence of a previously cloned 2-kb segment of *B. subtilis* DNA (contained in pOR100, Fig. 1) that included *cotE* and flanking DNA. This DNA was used as a starting point for a one-step chromosome walk in wild-type cells that extended about 10.5 kb in the direction of the origin of replication (see Materials and Methods). The resulting plasmid (pOR114, Fig. 1) contained an insert of 10.5 kb that extended 9 kb beyond *cotE*. When used to transform competent cells, pOR114 was able to correct the sporulation phenotype of the two suppressor mutations *spoVS*11-4 and *spoVS*9-4. As a control, we carried out an identical one-step chromosome walk with chromosomal DNA from the *spoVS*11-4 mutant. The resulting plasmid, pOR162 (Fig. 1), was identical to pOR114 except for the possible presence of the suppressor mutation. Unlike pOR114, pOR162 could not correct the sporulation phenotype of *spoVS*11-4 mutant cells. We infer that the wild-type allele of *spoVS* is present in pOR114 and that the *spoVS* mutant allele is present in pOR162.

To localize *spoVS* further, we subcloned fragments from the pOR114 insert and tested (as above) whether the subcloned DNAs could correct the sporulation phenotype of the *spoVS* mutants. Only subclone pOR175 (which contained a *Pst*I-*Sac*I insert of 2 kb, Fig. 1) was able to correct the *spoVS*11-4 mutation, and in fact corrected both of the other *spoVS* mutations (*spoVS*8-9 and *spoVS*9-4). Further localization was achieved by creating a nested set of unidirectionally deleted DNAs by exonuclease III digestion from the *Ecl*I136 site (see Materials and Methods). These deleted DNAs were tested for their ability to correct the sporulation phenotype of the *spoVS* mutants. Plasmid 8-1 (Fig. 1) contained the smallest insert that was able to correct the three *spoVS* mutations. This analysis indicated that all or part of *spoVS* must be present in the interval between the endpoints of the inserts in plasmids 8-1 and 12-2.

Sequence analysis of the wild-type DNA across the interval between plasmids 8-1 and 12-2 and the surrounding DNA with plasmid 2-2 (Fig. 1) revealed an 86-codon ORF, the predicted product of which was highly hydrophobic (46 of 86 amino acids are hydrophobic) (Fig. 2) but did not show strong similarity to proteins in the databases. The putative AUG start codon was preceded by a sequence that strongly conformed to other *B.*

TABLE 2. Heat-resistant cell production by various mutants[a]

Strain	Relevant genotype	No. of cells/ml	
		Viable	Heat resistant
PY79	Wild type	7×10^8	5.25×10^8
OR732	*spoVS*8-9	1.75×10^8	5.6×10^6
OR733	*spoVS*9-4	2.3×10^8	2.45×10^7
OR734	*spoVS*11-4	2.05×10^8	3.95×10^6
PY79	Wild type	8×10^8	6.4×10^8
OR661	*spoVSΔspc*	4.7×10^8	2.12×10^6
OR683	*spoVSΔspc spoVG*::Tn*917 spoIIB-lacZΩcat*	5.05×10^8	1.06×10^6
OR125	*spoVG*::Tn*917 spoIIB-lacZΩcat*	2.5×10^8	2.9×10^4

[a] Cells were sporulated in DS medium for about 24 h at 37°C. They were serially diluted, and both viable cells and heat-resistant cells (following a heat treatment at 80°C for 15 min) were plated on DS agar and counted. The numbers represent the averages from at least two experiments.

subtilis Shine-Dalgarno sequences, both in its complementarity to the 3′ terminus of *B. subtilis* 16S RNA and in its distance from the translation initiation codon (23). Sequence analysis of the corresponding DNA from the three *spoVS* mutants showed that each mutant contained a distinct single-nucleotide substitution within the 86-codon ORF (inside the interval predicted by plasmids 8-1 and 12-2) which resulted in three different amino acid substitutions (*spoVS*8-9, an Ala-to-Thr substitution at codon 38; *spoVS*9-4, an Ala-to-Val substitution at codon 42; and *spoVS*11-4, an Ala-to-Thr substitution at codon 16). The finding that all three mutations are transition mutations is consistent with the fact that they were generated by mutagenesis with nitrosoguanidine (11).

Two other ORFs in the interval defined by plasmids 8-1 and 12-2 were candidates for *spoVS*. These were a 76-codon ORF in the same orientation as *spoVS* and a 66-codon ORF in the opposite orientation. It is unlikely that either of these ORFs is *spoVS* for three reasons. First, neither ORF is preceded by an obvious Shine-Dalgarno sequence. Second, and more important, the *spoVS*9-4 mutation, which caused an Ala-to-Val substitution in the inferred product of the 86-codon ORF, would not have altered the inferred products of either alternative ORF, causing a silent CAG (Gln) to CAA (Gln) substitution at codon 14 of the 66-codon ORF and a silent GGC (Gly) to GGT (Gly) substitution at codon 60 of the 76-codon ORF. Finally, the results of chromosomal integration experiments based on the use of pOR191 (Fig. 1 and Materials and Methods) are inconsistent with *spoVS*'s being the 76-codon ORF. Plasmid OR191 contains a 200-bp insert that is entirely contained within the 86-codon ORF but does contain the 3′ end of the 76-codon ORF. Integration of pOR191 by a single-reciprocal recombination event would therefore have been expected to disrupt the 86-codon ORF but leave the 76-codon ORF intact. Plasmid OR191-generated integrants were in fact impaired in sporulation (data not shown).

Phenotype of the *spoVS* null mutant. To determine the phenotype of a *spoVS* null mutant, we replaced the *Bcl*I-to-*Taq*I interval that contained the first 10 codons of the gene with a spectinomycin resistance gene (see Materials and Methods and Fig. 1) to create strain OR661. The heat resistance of sporulated cultures of the *spoVS* null mutant (OR661) was indistinguishable from that of the *spoVS*8-9 and *spoVS*11-4 mutants and 10-fold lower than that of the *spoVS*9-4 mutant (Table 2). As confirmation that the effects of the null mutation were due to the *spoVSΔ*::*spc* mutation and not to a polar effect on a downstream gene, the *spoVS* null mutation could be complemented by a wild-type copy of *spoVS* and 2 kb of flanking DNA inserted at the *amyE* locus (OR708) but not by an equivalent segment of DNA bearing the *spoVS*11-4 point mutation (OR710) (data not shown).

Characterization of *spoVS* mutant cells by electron microscopy revealed that the spore core of both sporangia and immature spores harvested after 24 h of growth was abnormal. In wild-type cells at this stage of development, most of the cells released are mature spores. In such spores (Fig. 3A), the spore core has a white appearance and is lacking in substructure as a result of spore dehydration, which occurs at about the fourth hour of sporulation. In contrast, the spore core of *spoVS* null mutant sporangia (Fig. 3D) and immature spores (Fig. 3B) appeared punctate, suggesting a lack of dehydration. Second, although both the mutant sporangia and immature spores had a coat and a cortex, which are diagnostic of stage V, the coat structure of *spoVS* mutant cells was misassembled. A wild-type spore coat is characterized by two tightly juxtaposed layers with distinctive structures: a lightly staining lamellar inner coat and a darkly staining outer coat (Fig. 3A). In contrast, the coats of *spoVS* mutant spores and sporangia (Fig. 3B and D) often appeared thin and lacking in electron density. Furthermore, in some cases a portion of the coat structure appeared to be bulging or peeling away from the rest of the coat (Fig. 3D, arrows). These characteristics are consistent with cells that are blocked at stage V of development, on which basis we designated the gene *spoVS*.

A triple mutant (OR683) which was created by insertion of the *spoVS* null mutation into cells doubly mutant for *spoVG* and *spoIIB* had a phenotype very similar to that of the *spoVS* single mutant, as judged by colony phenotype on DS medium, phase-contrast light microscopy, the heat resistance of sporulated cultures (Table 2), and electron microscopy (Fig. 3C and E). Thus, the *spoVS* null mutation allowed cells defective in *spoIIB* and *spoVG* to advance beyond their normal developmental block and reach the (late) stage at which *spoVS* is required for further development. Cells doubly mutant for *spoVS* and *spoVG* or *spoVS* and *spoIIB* had a phenotype very similar to that of the *spoVS* single mutant (data not shown).

Use of a transcriptional fusion to study the regulation of *spoVS*. The use of a transcriptional fusion of *E. coli lacZ* to *spoVS* demonstrated that the gene was expressed at a low level during growth and was induced at the start of sporulation (Fig. 4A). This expression was blocked in an *spo0H* mutant but not in *spoIIG* or *spoIIAC* mutant cells. Consistent with the idea that *spoVS* is under the control of the product of *spo0H*, the transcription factor σ^H, sequences preceding *spoVS* show a region of similarity to the consensus for σ^H-controlled promoters, the proposed −35 and −10 sequences being CAGGA and GAAT, respectively (Fig. 2) (10). Further evidence that *spoVS* is under the control of σ^H came from the use of cells engineered to produce σ^H during growth in response to the addition of IPTG (isopropylthiogalactopyranoside) (Fig. 4B).

Expression of *spoVS* was also monitored by Northern blot hybridization, which revealed the accumulation during sporulation of an mRNA large enough (about 400 nucleotides) to encompass that predicted from the size (258 bp) of the *spoVS* gene (Fig. 5, lanes 1 and 2). This RNA was absent in *spoVS* null mutant cells (Fig. 5, lanes 3 and 4).

DISCUSSION

We report the identification and characterization of an additional *spo* gene, herein designated *spoVS*, which is induced at

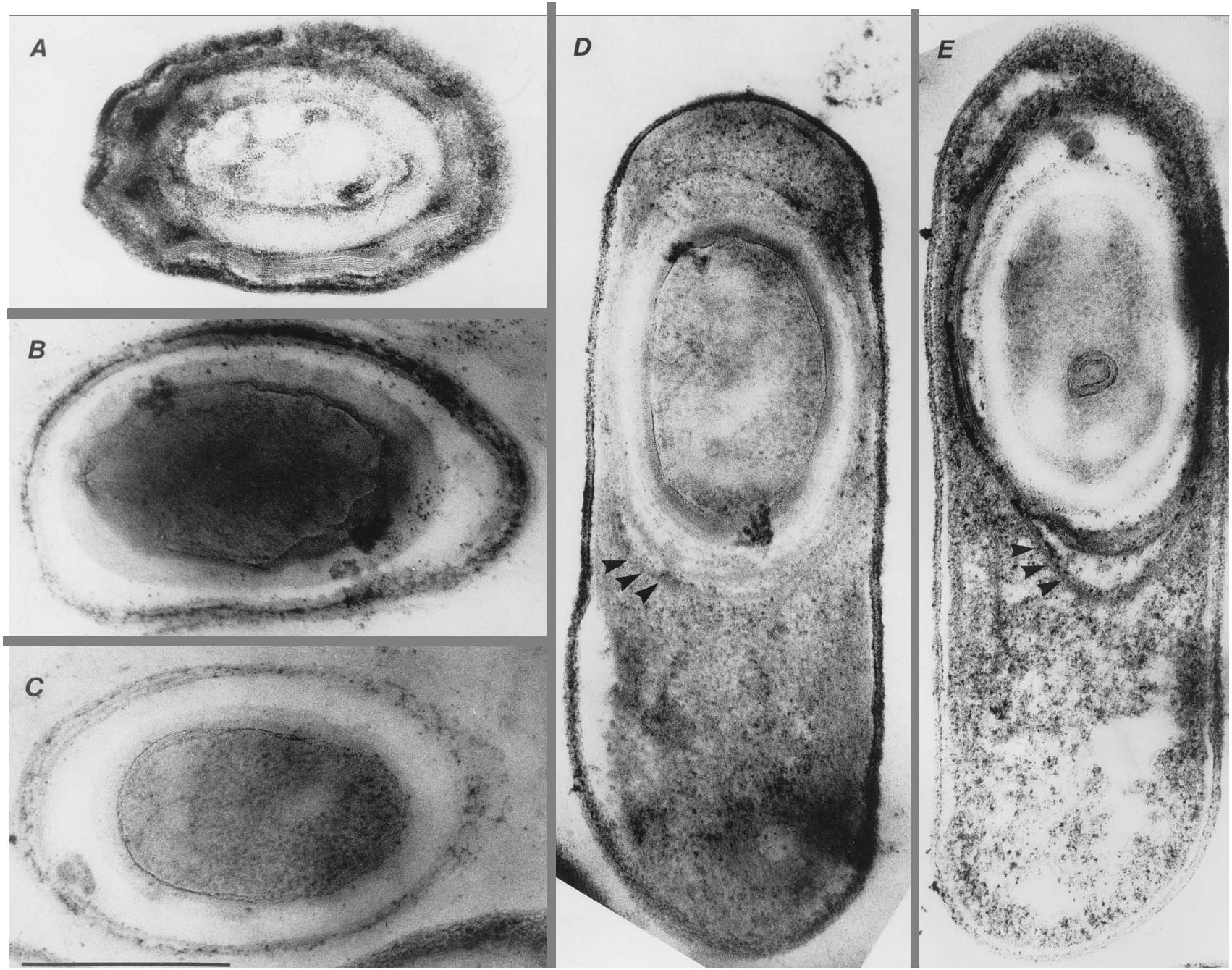

FIG. 3. Electron microscopy of spores and sporangia from *spoVS* mutant cells. (A) Wild-type spore from strain PY79; (B and C) spores from *spoVS* mutant strain OR661 (B) and *spoVS spoVG spoIIB* mutant strain OR683 (C); and (D and E) sporangium from *spoVS* mutant strain OR661 (D) and *spoVS spoVG spoIIB* mutant strain OR683 (E). Cells were grown to the 24th h of sporulation and then were fixed and sectioned for analysis by transmission electron microscopy as described previously (21). Bar, 500 nm.

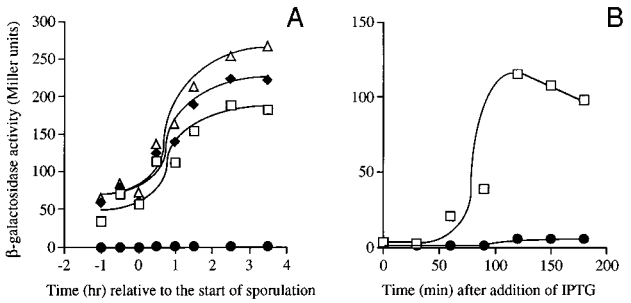

FIG. 4. (A) *spoVS*-directed β-galactosidase expression during growth and sporulation. Wild-type and mutant cells were grown in DS medium. Samples collected at the indicated times were assayed for β-galactosidase activity. The results are from *spoVS-lacZ*-bearing strains OR650 (*spo*$^+$, squares), OR652 (*spo0H*, circles), OR654 (*spoIIAC*, diamonds), and OR656 (*spoIIG*, triangles). (B) Induction of *spoVS-lacZ* during vegetative growth. A strain which carries a *spoVS-lacZ* fusion integrated at the *amyE* locus and *spo0H* under *spac* control (OR671) was grown in 2 × YT medium. When the optical density at 600 nm reached 0.3, the culture was divided, and IPTG was added to one of the cultures at 1 mM (squares); the other received no IPTG (circles). Samples collected at the indicated times were assayed for β-galactosidase activity.

the onset of sporulation under the control of σ^H. *spoVS* is 86 codons in length and is capable of encoding a protein of 8,796 Da which exhibits little similarity to other proteins in the databases. Null mutations in *spoVS* block sporulation at stage V, impairing the development of heat resistance and coat assembly.

Interestingly, loss-of-function mutations in *spoVS* cause two different, apparently contrasting phenotypes. In otherwise wild-type cells, the presence of a *spoVS* mutation impairs sporulation, reducing the level of heat-resistant cells by 100-fold. In contrast, the presence of a *spoVS* mutation in a *spoIIB spoVG* double mutant, which is blocked at stage II, allows sporulation to advance to a late stage. It may be noteworthy that, like *spoIIB* and *spoVG*, *spoVS* is under σ^H control (21, 36). Thus, all three gene products can be expected to appear at about the same time, prior to septum formation. Formally speaking, our results are consistent with the idea that wild-type SpoVS interferes with sporulation at an early stage and that this inhibitory effect is overcome by SpoIIB and SpoVG. On the other hand, SpoVS seems to play a positive role in allowing cells to progress beyond stage V of sporulation.

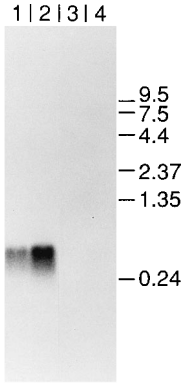

FIG. 5. Northern blot analysis of RNA from PY79 and *spoVS* mutant cells during sporulation. RNA was extracted from cells grown in DS medium and analyzed by Northern blot analysis. Lanes 1 and 3, samples taken at T_3; lanes 2 and 4, samples taken at T_5. Lanes 1 and 2, RNA from PY79 cells; lanes 3 and 4, RNA from OR661. RNA marker sizes are shown (in kilobases) on the right.

A clue as to the basis for the stage V block of a *spoVS* mutant is the observation in preliminary experiments that a *spoVS* mutation causes a substantial reduction in the level of expression of two genes, *cotA* (29) and *gerE* (6), that are under the control of the mother cell sigma factor σ^K (35). Because of the requirement for σ^K in cortex and coat formation (25), impairment of σ^K-directed gene expression could be a sufficient explanation for the effect of *spoVS* mutations in blocking sporulation at a late stage. The basis for the requirement for SpoVS to achieve high levels of σ^K activity is unknown.

How do *spoVS* mutations partially relieve the requirement for SpoIIB and SpoVG? Cells doubly mutant for *spoIIB* and *spoVG* are blocked at morphological stage II, producing a polar septum but retaining a thin layer of septal wall material, which is normally removed following septum formation in wild-type sporulating cells (13, 21). SpoIIB is believed to play a direct role in the removal of septal cell wall material, as its C-terminal region shows similarity to the C-terminal regions of certain cell wall hydrolases (15, 16, 21). The retention of the septal cell wall in a *spoIIB spoVG* mutant causes the septum to remain relatively rigid, evidently interfering with and preventing the subsequent process of engulfment (21). Somehow the absence of SpoVS allows dissolution of the septal wall to proceed. One way that this could occur would be if *spoVS* mutations cause sporulation to stall at stage II, allowing sufficient time for other, secondary cell wall hydrolase systems to degrade the peptidoglycan layer in the septum. Consistent with this idea, preliminary experiments indicate that *spoVS* mutations delay the onset of σ^E-directed gene transcription, as monitored by the expression of the *spoIVA* gene (28, 33). Such a timing effect would be reminiscent of the effect of a *kinA* mutation in delaying the expression of certain stage II genes and operons (1, 14) and of *bofA* and *bofB* mutations in advancing the time of expression of genes under the control of σ^K (5, 7, 27).

Although the precise function(s) of SpoVS remains obscure, our findings underscore the complexity of the process of septum formation and maturation and the delicate balance of physiological events taking place as cells progress through the septation, engulfment, and late stages of sporulation. Thus, as we have shown, *spoVS* mutations cause pleiotropic and contrasting effects early and late in development. A full understanding of the function of this newly discovered gene will require a detailed understanding of how it influences events occurring at distinct stages of morphogenesis.

ACKNOWLEDGMENTS

We thank P. Margolis for valuable discussions.

During a portion of this work, O.R. was supported by a fellowship from the Bunting Institute of Radcliffe College. This work was supported by NIH grant GM18568 to R.L.

REFERENCES

1. **Antoniewski, C., B. Savelli, and P. Stragier.** 1990. The *spoIIJ* gene, which regulates early developmental steps in *Bacillus subtilis*, belongs to a class of environmentally responsive genes. J. Bacteriol. **172:**86–93.
2. **Chen, N.-Y., S.-Q. Jiang, D. A. Klein, and H. Paulus.** 1993. Organization and nucleotide sequence of the *Bacillus subtilis* diaminopimelate operon, a cluster of genes encoding the first three enzymes of diaminopimelate synthesis and dipicolinate synthase. J. Biol. Chem. **268:**9448–9465.
3. **Chung, C. T., S. L. Niemela, and R. H. Miller.** 1989. One-step preparation of competent *Escherichia coli*: transformation and storage of bacterial cells in the same solution. Proc. Natl. Acad. Sci. USA **86:**2172–2175.
4. **Coote, J. G.** 1972. Sporulation in *Bacillus subtilis*: characterization of oligosporogenous mutants and comparison of their phenotypes with those of asporogenous mutants. J. Gen. Microbiol. **71:**1–15.
5. **Cutting, S., V. Oke, A. Driks, R. Losick, S. Lu, and L. Kroos.** 1990. A forespore checkpoint for mother cell gene expression during development in *B. subtilis*. Cell **62:**239–250.

6. **Cutting, S., S. Panzer, and R. Losick.** 1989. Regulatory studies on the promoter for a gene governing synthesis and assembly of the spore coat in *Bacillus subtilis*. J. Mol. Biol. **207:**393–404.
7. **Cutting, S., S. Roels, and R. Losick.** 1991. Sporulation operon *spoIVF* and the characterization of mutations that uncouple mother cell from forespore gene expression in *Bacillus subtilis*. J. Mol. Biol. **221:**1237–1256.
8. **Dubnau, D., and R. Davidoff-Abelson.** 1971. Fate of transforming DNA following uptake by competent *B. subtilis*. J. Mol. Biol. **56:**209–221.
9. **Frandsen, N., and P. Stragier.** 1995. Identification and characterization of the *Bacillus subtilis spoIIP* locus. J. Bacteriol. **177:**716–722.
10. **Gross, C. A., M. Lonetto, and R. Losick.** 1992. Bacterial sigma factors, p. 131. *In* S. L. McKnight and K. R. Yamamoto (ed.), Transcriptional regulation, vol. 1. Cold Spring Harbor Laboratory Press, Cold Spring Harbor, N.Y.
11. **Harwood, C. R., and S. M. Cutting.** 1990. Molecular biological methods for Bacillus. John Wiley & Sons, New York.
12. **Hudspeth, D. S. S., and P. S. Vary.** 1992. *spoVG* sequence of *Bacillus megaterium* and *Bacillus subtilis*. Biochim. Biophys. Acta **1130:**229–230.
13. **Illing, N., and J. Errington.** 1991. Genetic regulation of morphogenesis in *Bacillus subtilis*: role of sigma E and sigma F in prespore engulfment. J. Bacteriol. **173:**3159–3169.
14. **Ireton, K., and A. D. Grossman.** 1992. Interactions among mutations that cause altered timing of expression during sporulation in *Bacillus subtilis*. J. Bacteriol. **174:**3185–3195.
15. **Kuroda, A., Y. Asami, and J. Sekiguchi.** 1993. Molecular cloning of a sporulation-specific cell wall hydrolase gene of *Bacillus subtilis*. J. Bacteriol. **175:** 6260–6268.
16. **Kuroda, A., Y. Sugimoto, T. Funahashi, and J. Sekiguchi.** 1992. Genetic structure, isolation and characterization of a *Bacillus licheniformis* cell wall hydrolase. Mol. Gen. Genet. **234:**129–137.
17. **LeDeaux, J. R., and A. D. Grossman.** 1995. Isolation and characterization of *kinC*, a gene that encodes a sensor kinase homologous to the sporulation sensor kinases KinA and KinB in *Bacillus subtilis*. J. Bacteriol. **177:**166–175.
18. **Losick, R., P. Youngman, and P. J. Piggot.** 1986. Genetics of endospore formation in *Bacillus subtilis*. Annu. Rev. Genet. **20:**625–669.
19. **Maniatis, T., E. F. Fritsch, and J. Sambrook.** 1982. Molecular cloning: a laboratory manual. Cold Spring Harbor Laboratory, Cold Spring Harbor, N.Y.
20. **Margolis, P., A. Driks, and R. Losick.** 1991. Establishment of cell type by compartmentalized activation of a developmental transcription factor. Science **254:**562–565.
21. **Margolis, P. S., A. Driks, and R. Losick.** 1993. Sporulation gene *spoIIB* from *Bacillus subtilis*. J. Bacteriol. **175:**528–540.
22. **Miller, J. H.** 1972. Experiments in molecular genetics, p. 354. Cold Spring Harbor Laboratory, Cold Spring Harbor, N.Y.
23. **Moran, C. P., Jr., N. Lang, S. F. J. LeGrice, G. Lee, M. Stephens, A. L. Sonenshein, J. Pero, and R. Losick.** 1982. Nucleotide sequences that signal the initiation of transcription and translation in *Bacillus subtilis*. Mol. Gen. Genet. **186:**339–346.
24. **Peacock, A. C., and C. W. Dingman.** 1967. Resolution of multiple ribonucleic acid species by polyacrylamide gel electrophoresis. Biochemistry **6:**1818–1827.
25. **Piggot, P. J., and J. G. Coote.** 1976. Genetic aspects of bacterial endospore formation. Bacteriol. Rev. **40:**908–962.
26. **Resnekov, O., L. Rutberg, and A. von Gabain.** 1990. Changes in the stability of specific mRNA species in response to growth stage in *Bacillus subtilis*. Proc. Natl. Acad. Sci. USA **87:**8355–8359.
27. **Ricca, E., S. Cutting, and R. Losick.** 1992. Characterization of *bofA*, a gene involved in intercompartmental regulation of pro-σK processing during sporulation in *Bacillus subtilis*. J. Bacteriol. **174:**3177–3184.
28. **Roels, S., A. Driks, and R. Losick.** 1992. Characterization of *spoIVA*, a sporulation gene involved in coat morphogenesis in *Bacillus subtilis*. J. Bacteriol. **174:**575–585.
29. **Sandman, K., L. Kroos, S. Cutting, P. Youngman, and R. Losick.** 1988. Identification of the promoter for a spore coat protein gene in *Bacillus subtilis* and studies on the regulation of its induction at a late stage in sporulation. J. Mol. Biol. **200:**461–473.
30. **Sandman, K., R. Losick, and P. Youngman.** 1987. Genetic analysis of *Bacillus subtilis spo* mutations generated by Tn*917*-mediated insertional mutagenesis. Genetics **117:**603–617.
31. **Sanger, F., S. Nicklen, and A. R. Coulson.** 1977. DNA sequencing with chain-terminating inhibitors. Proc. Natl. Acad. Sci. USA **74:**5463–5467.
32. **Smith, K., M. E. Bayer, and P. Youngman.** 1993. Physical and functional characterization of the *Bacillus subtilis spoIIM* gene. J. Bacteriol. **175:**3607–3617.
33. **Stevens, C. M., R. Daniel, N. Illing, and J. Errington.** 1992. Characterization of a sporulation gene, *spoIVA*, involved in spore coat morphogenesis in *Bacillus subtilis*. J. Bacteriol. **174:**586–594.
34. **Vandeyar, M. A., and S. A. Zahler.** 1986. Chromosomal insertions of Tn*917* in *Bacillus subtilis*. J. Bacteriol. **167:**530–534.
35. **Zheng, L., W. P. Donovan, P. C. Fitz-James, and R. Losick.** 1988. Gene encoding a morphological protein required in the assembly of the outer coat of the *Bacillus subtilis* endospore. Genes Dev. **2:**1047–1054.
36. **Zuber, P., and R. Losick.** 1983. Use of a *lacZ* fusion to study the role of the *spo0* genes of *Bacillus subtilis* in developmental regulation. Cell **35:**275–283.